

## The effect of strain rate in DP steels and the three stages of work hardening

### Introduction

In the early 1930<sup>th</sup> Taylor(1), Polanyi(2) and Orowan(3) almost contemporarily realized that the plastic deformation of crystalline materials could be explained in terms of the dislocation theory proposed by Volterra(4) in 1905. This insight has proved to be critical for the development of the mechanical properties of modern metals and alloys. The dislocation theory together with transmission electron microscopy (TEM) and the Taylor theory for work hardening (5) have been invaluable tools in the increased understanding of the complex work hardening process. These scientists were exceptional in the sense that they had both the ability and the courage to break new ways. It seems, however, that the progress in this important area of material physics has slowed down markedly over the last decades at least if we look at the number of attempts made to develop new physically based dislocation theories for work hardening. This seems a little bizarre when we at the same time notice an exceptional progress in other fields in the society like computers, communication and internet for example. It also seems to be a tendency among scientists to-day to by-pass and neglect areas dealing with the basic physical mechanisms involved in the plastic deformation process. This was also pointed out by Mughrabi (6) who stated that: "The increasing number of SGP (strain gradient plasticity) theories confirms that the search for a really satisfactory theory is still going on. Better micro structurally founded physical models should be pursued with priority before further development of rather formal, generalized concepts in which the physics tends to be hidden".

The problems involved in the work hardening behavior of single-phase metals are still complex and even more so in metals containing several phases. It has been known for a long time that the deformation process is inhomogeneous not only in multi-phase materials but also in single-phase ones. In-situ TEM-studies of single-phase materials show that only a certain fraction of the grains undergo plastic deformation in the initial stages (7). However, as the strain increases, also the remaining grains successively start to take part in the deformation process (8). Similar observations have been made in dual-phase steel in which the hard martensite does not deform plastically for strains below that of necking (9). It also holds for this type of steels that the ferrite deforms inhomogeneously in such a way that deformation starts in the ferrite close to the martensite boundaries and then progresses inwards the ferrite (9)-(11). This implies that the local strain in the ferrite is much larger than that evaluated from a standard uniaxial tensile test.

Unfortunately, very few attempts have been made to take the inhomogeneous behavior into account when formulating theories for inhomogeneous materials like DP steel which, of course, will lead to misleading results and uncertain conclusions. The idea proposed by Ashby (12) of geometrical and statistical dislocations where the geometrical dislocations are formed by pile-ups of dislocations is unrealistic for ferrite because of the high stacking fault energy and the great number of slip systems in this structure.

In a recent paper, however, Bergström et al (13) present a dislocation-based model for DP – steel valid for strains up to necking. This model is based on the assumption that the plastic deformation process is inhomogeneous in the sense that it is located to the soft ferrite phase at least up to necking. It is also assumed that the plastic deformation in the ferrite progresses inhomogeneously.

These assumptions are supported by experiments (8, 13) and Bergström et al (13) show that the theory in a convincing way can describe the true stress – strain behavior of different types of DP steels for strains up to necking.

A key parameter in the proposed theory is the strain dependent in-homogeneity factor,  $f(\varepsilon)$ , which describes the strain dependence of the volume fraction of ferrite taking active part in the plastic deformation process. Initially, this volume fraction is small but increases with increasing strain towards a final value equal to the total volume fraction of ferrite.

This, of course, results in a strain dependent strain rate in the active volume fraction of ferrite and causes the thermal friction stress to decrease with strain. This was not taken into account in the original paper (13). Now, since it is the objective of the present paper to investigate how strain-rate affects the work hardening behavior of DP600 steel, we will extend the model to incorporate the strain dependence of the thermal stress.

It is also the objective of the present work to establish how a changing strain rate affects the various physical parameters involved in the model. Furthermore, an attempt is made to estimate the temperature increase in the tensile test specimens during testing via the fitting process.

## THEORY

### *A brief review of the recently presented dislocation model for DP steel*

The relation between the true flow stress,  $\sigma(\varepsilon)$ , and the total dislocation density,  $\rho(\varepsilon)$ , may according to Taylor (5) be written:

$$\sigma(\varepsilon) = \sigma_{i0} + \alpha \cdot G \cdot b \cdot \rho(\varepsilon)^{\frac{1}{2}} \quad (1)$$

where  $\varepsilon$  is the true strain,  $\sigma_{i0}$  is the friction stress,  $\alpha$  is a dislocation strengthening parameter,  $G$  is the shear modulus and  $b$  is the nominal value of the Burgers vector.

The strain dependence of the total dislocation density,  $\rho(\varepsilon)$ , in DP – steel may according to Bergström et al (13) be written

$$\frac{d\rho(\varepsilon)}{d\varepsilon} = \frac{1}{f(\varepsilon)} \cdot \left[ \frac{m}{b \cdot s(\varepsilon)} - \Omega \cdot \rho(\varepsilon) \right] \quad (2)$$

where  $f(\varepsilon)$  is the volume fraction of ferrite taking active part in the plastic deformation process,  $s(\varepsilon)$  is the mean free path of dislocation motion and  $\Omega$  is the dislocation remobilisation parameter. It is assumed, in accordance with experimental observations, that  $f(\varepsilon)$  increases with strain in the following way (13)

$$f(\varepsilon) = f_0 + (f_1 - f_0) \cdot e^{-r \cdot \varepsilon} \quad (3)$$

where  $f_1$  is the initial active volume fraction,  $f_0$  the final active volume fraction and  $r$  is a material dependent rate constant. This means that  $f(\varepsilon)$  increases with strain from a start value of  $f_1$  to a final value of  $f_0$  in accordance with the law of natural growth. The mean free path  $s(\varepsilon)$  of dislocation motion is according to a similar reasoning assumed to decrease with strain as (13)

$$s(\varepsilon) = s_0 + (s_1 - s_0) \cdot e^{-k \cdot \varepsilon} \quad (4)$$

where  $s_1$  is the initial mean free path and  $s_0$  the final one.  $k$  is a material dependent rate constant.

In ferrite the friction stress,  $\sigma_{i0}$ , may be split up into a thermally independent component,  $\sigma_{at}$ , and a thermal component,  $\sigma^*$ , that is

$$\sigma_{i0} = \sigma_{at} + \sigma^* \quad (5a)$$

Here the non thermal component  $\sigma_{at}$  may be split up into the following components

$$\sigma_{at} = \sigma_g + \sigma_p + \sigma_s \quad (5b)$$

where the components in turn stand for grain-size hardening, precipitation hardening and solution hardening.

Previous studies have shown that  $\sigma^*$  for a ferrite steel may be written (7, 8)

$$\sigma^* = \sigma_0 \cdot \left( \frac{\dot{\varepsilon}_0}{\nu} \right)^{\frac{T}{T_0}} \quad (6)$$

where  $\sigma_0$ ,  $\nu$  and  $T_0$  are material constants,  $\dot{\varepsilon}_0$ , is the applied strain rate and  $T$  is the temperature in K.

In the present case when dealing with a DP steel, where the active volume fraction,  $f(\varepsilon)$ , varies with strain we must also take into account the fact that the strain rate in the local volume varies with strain in the following way

$$\dot{\varepsilon}(\varepsilon) = \frac{\dot{\varepsilon}_0}{f_0 + (f_1 - f_0) \cdot e^{-r \cdot \varepsilon}} \quad (7)$$

The strain dependence of the thermal friction stress in the local volume taking part in the plastic deformation process may therefore, in accordance with eqn. (6) and (7), be written

$$\sigma^*(\varepsilon) = \sigma_0 \cdot \left( \frac{1}{\nu} \frac{\dot{\varepsilon}_0}{f_0 + (f_1 - f_0) \cdot e^{-r \cdot \varepsilon}} \right)^{\frac{T}{T_0}} \quad (8)$$

Proceeding from equations (1) – (8) we may now via integration fit these relationships to experimental stress – strain data. This opens for a new way to analyze the mechanisms behind the plastic deformation process in DP steel and how this process is affected by strain and strain rate.

### Experimental

A commercially produced DP600 steel of the composition presented in Table 1 was tensile tested at room temperature and at various strain rates in the range  $0,0000779 \text{ s}^{-1}$ –  $0,0467 \text{ s}^{-1}$ .

Table 1. Chemical composition

C	Mn	Si	Nb	P	S	Al	Ti	B	N	V
0,112	0,89	0,45	0,001	0,012	0,003	0,04	0,001	0,0002	0,0027	0,013

In the study a total of eight strain rates were applied with two tests being carried out at each strain rate. True plastic stress – strain curves were evaluated and some examples are shown in Fig. 1. There are no signs of the Lüders effect on the curves and it is apparent that the hardness and rate of strain hardening are slightly affected by variations in strain rate.

In the investigated material the volume fraction of martensite is experimentally estimated to be approximately 17%. This implies that the volume fraction of ferrite is approximately equal to 83%.

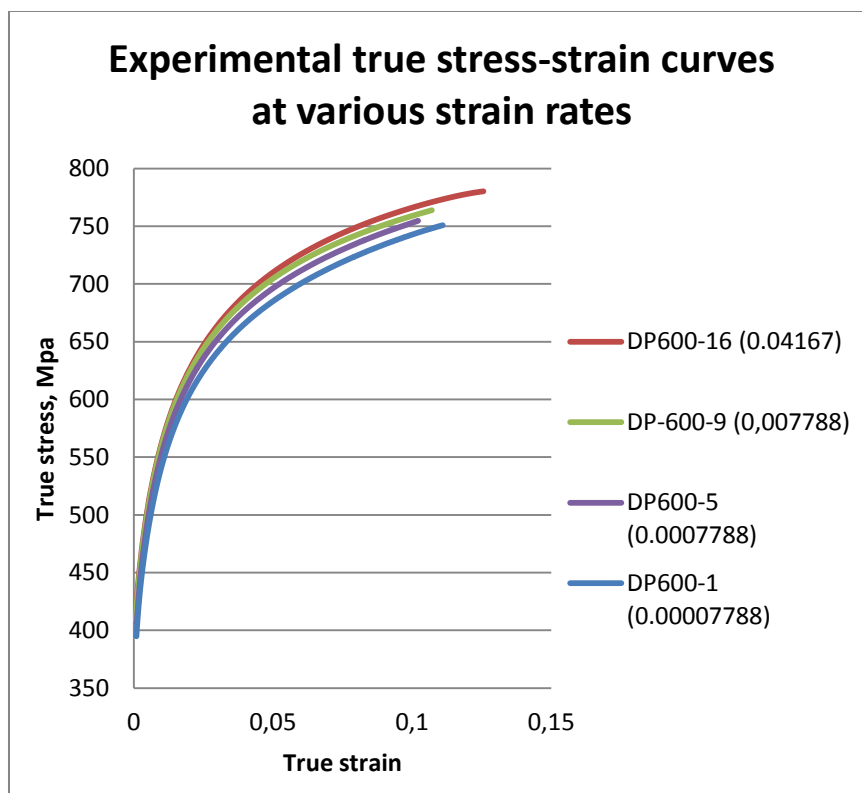


Fig. 1. Examples of experimental  $\sigma$ - $\epsilon$  curves recorded at room temperature and at 4 different strain rates namely DP600-1 ( $4,2 \cdot 10^{-4} \text{ s}^{-1}$ ), DP600-5 ( $4,2 \cdot 10^{-3} \text{ s}^{-1}$ ), DP600-9 ( $4,2 \cdot 10^{-2} \text{ s}^{-1}$ ), DP600-19 ( $7,8 \cdot 10^{-5} \text{ s}^{-1}$ )

### Fitting of the model to experimental stress-strain data

In fitting the model to experimental stress-strain curves we will use a specially designed subroutine based on the Matlab Curve Fitting Toolbox. The following parameters are kept constant in the fitting procedure:  $\alpha=0.5$ ,  $G=80000\text{MPa}$ ,  $b=2.5\cdot 10^{-10}\text{ m}$ ,  $m=2$ ,  $\sigma_0=1000\text{ MPa}$ ,  $T_0=2680\text{ K}$ ,  $v=1\cdot 10^9\text{ s}^{-1}$  and  $\dot{\epsilon}_0 = (0.0000779 - 0.0467)\text{ s}^{-1}$ . The other parameters in the model are allowed to vary freely within physically reasonable values. The choice of start values is based on experience.

During plastic deformation mechanical work is produced and most of this energy is transformed into heat. We will therefore allow the specimen temperature  $T$  to vary freely in order to check whether the theory is capable of estimating the local temperature inside the tested specimen. An attempt will also be made to estimate the value of  $T$  proceeding from the energy input into the specimen via the experimental stress-strain curve. A comparison between the two types of results will be made.

The result from a fit of the model to an experimental stress-strain curve tested at RT and an applied strain-rate of  $0.0000779\text{ s}^{-1}$  is presented in Fig. 2. To the left on the upper half of the graph we can see the experimental  $\sigma$ - $\epsilon$  curve and the superimposed fitted curve. The theory predicts a true strain to necking of 10.8% and a corresponding flow stress equal to 749.3 MPa. These values are in good agreement with those experimentally observed.  $Z=1$  stands for uniaxial tension.

Method: TMP - Date: 2011-11-04 - Time: 12:39 - Data file name: DP600-190000, Prov-1.txt - Data file path: C:\Users\yngve-ny\Desktop\DP600-slutanalys\

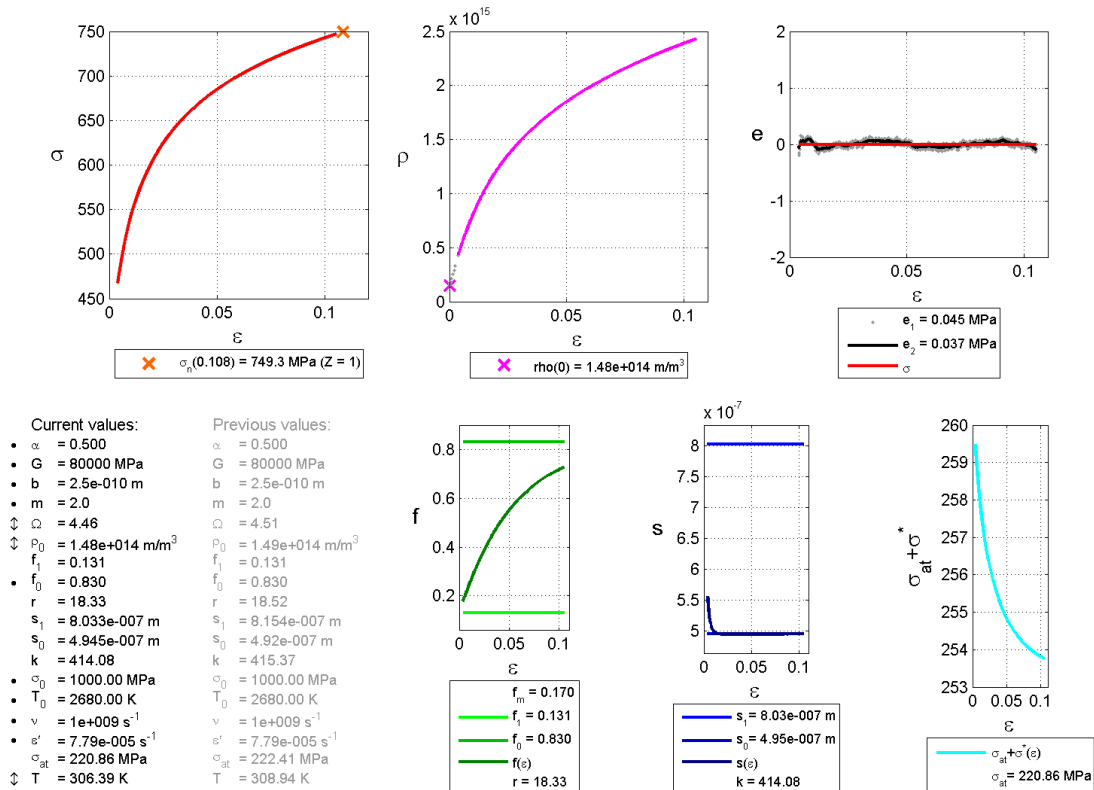


Fig. 2. The results obtained by fitting the dislocation model to a uniaxial  $\sigma$ - $\epsilon$  curve from DP600 steel.  $T=296\text{ K}$  and  $\dot{\epsilon}_0=0.000417\text{ s}^{-1}$ , see text.

In the upper middle graph the corresponding  $\rho$ - $\epsilon$  curve is presented and the results indicate that the “grown-in” dislocation density,  $\rho_0$ , takes a value of  $1.48 \cdot 10^{14} \text{ m}^{-2}$ . This  $\rho_0$  – value together with a  $\Omega$ -value equal to 4.46 are normal values for ferrite in DP600 steel.

In the upper right graph the errors in the fit are shown and the max-value is estimated to be less than approximately 0.25 MPa. The statistical errors  $e_1$  and  $e_2$  are considerably smaller.

The table in the lower left graph shows the parameter values. The black dots in front of some of the parameters indicate that those parameters are kept constant during the fitting process. The arrows in front of some other parameters indicate that these parameters are changing in smaller steps in the fitting process.

The graphs to the lower right in Fig. 2 show in turn the strain dependences of  $f(\epsilon)$ ,  $s(\epsilon)$  and  $\sigma_{10}(\epsilon)$ . The total volume fraction of martensite has in accordance with experimental observations been put equal to 17%.

The initial volume fraction of active ferrite,  $f_1$ , is calculated to be 13.1% and its final value is put equal to  $f_0=83\%$  since the martensite content is 17%. Since the rate constant  $r$  takes the rather low value of 18.3 the strain to reach  $f_0$  is high and approximately equal to 15%. At the strain to necking  $f$  is equal to approximately 70% active ferrite, se Fig. 2.

The mean free path,  $s(\epsilon)$ , of the mobile dislocations located in the active volume fraction, takes the initial value of  $s_1 \approx 0.8 \text{ }\mu\text{m}$  and, as strain increases, reaches its final value of  $s_0 \approx 0.49 \text{ }\mu\text{m}$  already after approximately 1% of strain because of the high value of  $k=414$ .

Table 2. Parameter values obtained by fitting the proposed theory to experimental uniaxial stress-strain curves recorded from DP600 steel. Testing temperature  $T=296\text{K}$  and the applied strain rate,  $\dot{\epsilon}_0$ , varies in the range  $0.000417 \text{ s}^{-1} - 0.417 \text{ s}^{-1}$ .

Test	$\dot{\epsilon}_0 \text{ (s}^{-1}\text{)}$	$\rho_0 \text{ (m}^{-2}\text{)}$	$f_1$	$r$	$s_1 \text{ (m)}$	$s_0 \text{ (m)}$	$k$	$\sigma_{at} \text{ (MPa)}$	T(K)	$\Omega$
DP600-1	0.0000779	$1.48 \cdot 10^{14}$	0.131	18.33	$8.03 \cdot 10^{-7}$	$4.95 \cdot 10^{-7}$	414.1	220.9	306.4	4.46
DP600-3	0.000156	$1.56 \cdot 10^{14}$	0.117	19.59	$7.54 \cdot 10^{-7}$	$4.75 \cdot 10^{-7}$	378.2	219.9	310.9	4.64
DP600-4	0.000156	$1.57 \cdot 10^{14}$	0.117	19.59	$7.64 \cdot 10^{-7}$	$4.76 \cdot 10^{-7}$	372.7	218.2	307.9	4.54
DP600-5	0.000779	$1.54 \cdot 10^{14}$	0.142	16.91	$7.30 \cdot 10^{-7}$	$4.74 \cdot 10^{-7}$	573.6	211.2	300.8	4.72
DP600-6	0.000779	$1.56 \cdot 10^{14}$	0.146	17.96	$8.75 \cdot 10^{-7}$	$4.72 \cdot 10^{-7}$	574.3	217.4	301.6	4.85
DP600-7	0.00156	$1.72 \cdot 10^{14}$	0.155	17.36	$8.03 \cdot 10^{-7}$	$4.70 \cdot 10^{-7}$	558.2	220.4	303.9	5.07
DP600-8	0.00156	$1.73 \cdot 10^{14}$	0.161	17.96	$7.81 \cdot 10^{-7}$	$4.66 \cdot 10^{-7}$	516.6	220.4	300.8	5.14
DP600-9	0.00779	$1.60 \cdot 10^{14}$	0.176	15.18	$1.38 \cdot 10^{-6}$	$4.81 \cdot 10^{-7}$	910.6	231.7	310.4	5.4
DP600-10	0.00779	$1.61 \cdot 10^{14}$	0.182	14.68	$1.44 \cdot 10^{-6}$	$4.78 \cdot 10^{-7}$	879.2	234.6	314.2	5.48
DP600-11	0.0156	$1.64 \cdot 10^{14}$	0.186	14.1	$1.63 \cdot 10^{-6}$	$4.84 \cdot 10^{-7}$	1012.1	229.1	307.5	5.41
DP600-12	0.0156	$1.65 \cdot 10^{14}$	0.195	13.93	$1.41 \cdot 10^{-6}$	$4.87 \cdot 10^{-7}$	948.5	226.2	303.6	5.32
DP600-13	0.0312	$1.60 \cdot 10^{14}$	0.193	13.5	$2.95 \cdot 10^{-6}$	$4.99 \cdot 10^{-7}$	1321.5	232.4	307.0	5.36
DP600-14	0.0312	$1.60 \cdot 10^{14}$	0.202	13.01	$3.08 \cdot 10^{-6}$	$4.98 \cdot 10^{-7}$	1375.6	235.6	307.0	5.43
DP600-15	0.0467	$1.54 \cdot 10^{14}$	0.202	13.53	$3.48 \cdot 10^{-6}$	$4.74 \cdot 10^{-7}$	1791.7	222.8	301.8	5.53
DP600-16	0.0467	$1.55 \cdot 10^{14}$	0.205	14.11	$3.36 \cdot 10^{-6}$	$4.72 \cdot 10^{-7}$	1795.3	232.2	318.6	5.5
<b>Mean value</b>		<b><math>1.6 \cdot 10^{14}</math></b>				<b>0.48</b>		<b>224.88</b>	<b>306.8</b>	<b>5.12</b>
Stand.dev.		$\pm 0.05 \cdot 10^{14}$				$\pm 0.009 \text{ }\mu\text{m}$		$\pm 6.37$	$\pm 3.86$	$\pm 0.33$

The graph to the right in the lower part of Fig. 2 shows the strain dependence of the friction stress,  $\sigma_{i0}$ , and it is clear that the athermal component,  $\sigma_{at} \approx 224,9$  MPa while the thermal part,  $\sigma^*$ , decreases with elongation.

All experimental  $\sigma$ - $\epsilon$  curves were analyzed in a similar manner and the results obtained are presented in Table 2. Here also the values for the theoretically estimated testing specimen temperature, T K, see eqn.(8), is presented together with the recorded  $\Omega$  – values. The mean value of T is estimated to be  $306.8 \pm 3.9$  K and that for  $\Omega \approx 5.12 \pm 0.33$  see Table 2. The “grown-in” dislocation density  $\rho_0$  takes a value approximately equal to  $1.6 \cdot 10^{14} \pm 0.05 \cdot 10^{14} \text{ m}^{-2}$ .

### Analysis and discussion

In the proposed theory the “grown-in” dislocation density,  $\rho_0$ , the volume fraction of ferrite,  $f_0$ , and the athermal friction stress,  $\sigma_{at}$ , are, on a physical basis, assumed to be independent of strain and strain rate and this is also in accordance with the results presented in Table 2. There we can also see that  $s_0$  as well as  $\Omega$  and T remain rather independent of strain-rate - at least within the present experimental frames - with average values equal to  $0.48 \pm 0.01 \mu\text{m}$ ,  $5.12 \pm 0.33$  and  $306.8 \pm 3.9$  K respectively.

It is well known that the plastic true stress-strain curves of DP steels can be divided into three different stages (10) and we will present a physical explanation for this behavior by analyzing the strain behaviors of  $\dot{\epsilon}(\epsilon)$ ,  $f(\epsilon)$  and  $s(\epsilon)$ .

The parameters defining the factors  $\sigma^*(\epsilon)$ ,  $f(\epsilon)$  and  $s(\epsilon)$ , exhibit a certain strain-rate dependence and we will start by discussing these parameters.

### The effect of strain rate on work hardening in DP600 steel

#### **Local strain rate $\dot{\epsilon}(\epsilon)$ and thermal friction stress $\sigma^*(\epsilon)$**

It is assumed in the present theory that the plastic deformation process is located to a strain dependent active volume fraction,  $f(\epsilon)$ . Now, since  $f(\epsilon)$  is growing with increasing strain the result will be that both the local strain rate  $\dot{\epsilon}(\epsilon)$  and the corresponding thermal component,  $\sigma^*(\epsilon)$ , will diminish with increasing strain, see Fig. 3a and 3b. At the highest applied strain rate the local strain rate  $\dot{\epsilon}(\epsilon)$  decreases from a value of ca  $0.23 \text{ s}^{-1}$  at zero strain to a value of ca  $0.05 \text{ s}^{-1}$  at 20% of strain. At the two smallest applied strain rates the effects are almost negligible.

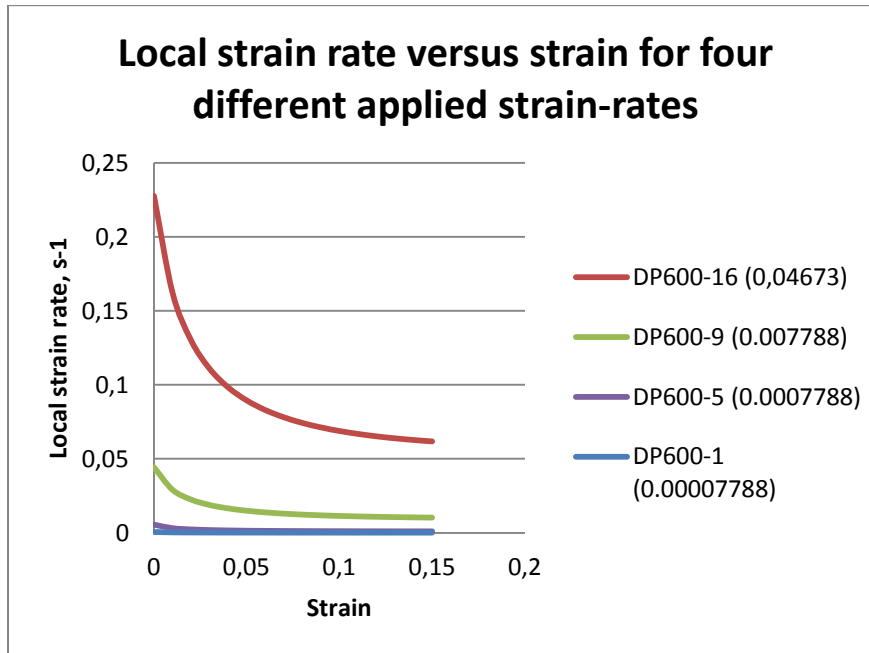


Fig. 3a. Local strain rate,  $\dot{\epsilon}(\epsilon)$ , versus strain at four different applied strain rates.

The decrease in  $\sigma^*(\epsilon)$  with strain is in the range 10 MPa at the highest strain rate which illustrates the necessity to take the strain rate variation into account in a detailed analysis. In harder DP steels with a higher volume content of martensite the effect will be more pronounced and we will return to this in a forthcoming paper. In the latter types of steel even the ductility of the material might be reduced due to the decreasing thermal friction stress with strain and a resulting decreasing strain to necking.

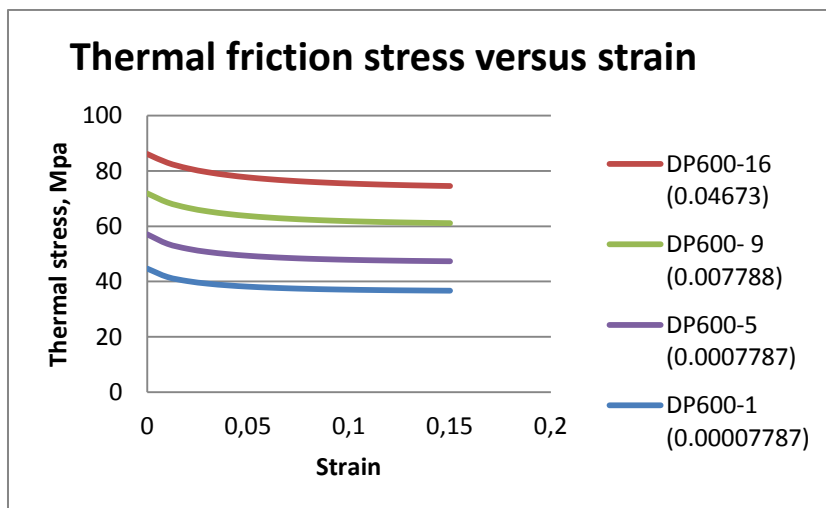


Fig. 3b. Local thermal friction stress  $\sigma^*(\epsilon)$ , versus strain at four different applied strain rates. The decrease in  $\sigma^*(\epsilon)$  with increasing strain is in the range 5 -10 MPa.

#### The volume fraction $f(\epsilon)$ :

Initial volume fraction,  $f_1$

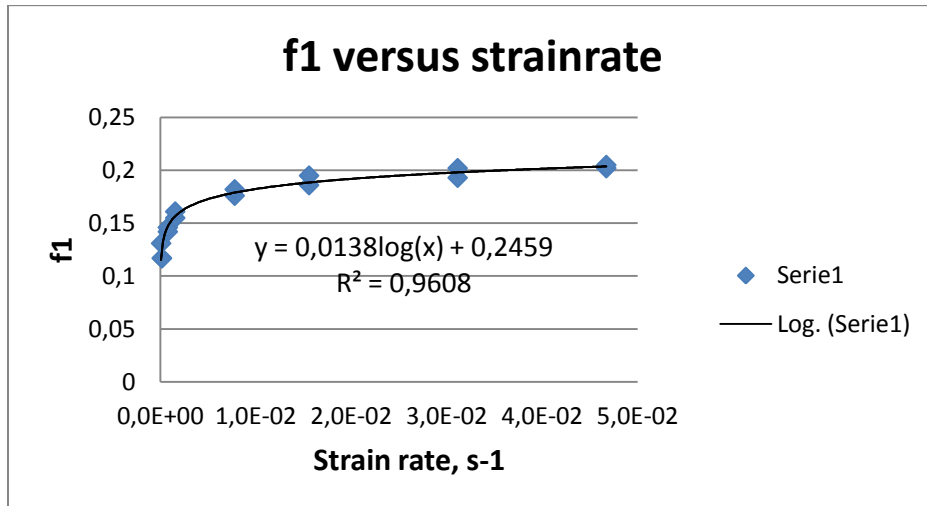


Fig.4. a.  $f_1$  versus applied strain rate at  $T=296K$ . (See Table 2)

According to eqn.(3) it holds that the active volume fraction,  $f(\epsilon)$ , increases with strain from an initial value  $f_1$  to a final value  $f_0$  at a rate defined by the rate constant  $r$ . Here  $f_0$  is strain rate independent while, according to Table 2,  $f_1$  and  $r$  vary with strain rate.  $f_1$  stands for the initial volume fraction of ferrite taking part in the plastic deformation process and it is reasonable to assume that its value to some extent is influenced by tensile residual stresses and various types of initial stress concentrators. A plot of  $f_1$  versus the applied strain rate  $\dot{\epsilon}_0$  is shown in Fig. 4a and the result indicates that, at the highest applied strain rate,  $f_1$  increases with  $\dot{\epsilon}_0$  from a value of approximately 0.1 to a value of approximately 0.2. This increase may be expressed mathematically by the following expression, see Fig. 4a

$$f_1 = 0.0138 \cdot \log(\dot{\epsilon}_0) + 0.2459 \quad (9)$$

Since thermal activation will decrease with increasing applied strain rate a larger initial active volume fraction of ferrite is obviously needed to keep the plastic deformation process going.

#### The rate constant $r$

The parameter  $r$  is a measure of the rate by which the active volume fraction of ferrite grows with enhanced strain and the fitting procedure results in the following relationship between  $r$  and applied strain rate,  $\dot{\epsilon}_0$

$$r = 10,229 - 1.67 \cdot \log(\dot{\epsilon}_0) \quad (10)$$

This indicates that  $r$  declines with increasing strain rate, see Fig. 4b, which also is to be expected when strain rate increases.

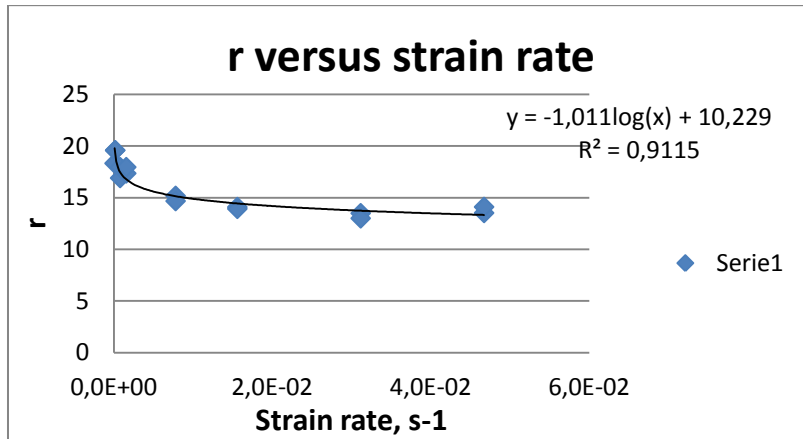


Fig. 4b. Rate constant  $r$  versus applied strain rate at  $T=296K$ .

### The mean free path of dislocation motion, $s(\epsilon)$

#### Initial mean free path $s_1$

While  $f(\epsilon)$  defines the expansion of the volume fraction of active ferrite,  $s(\epsilon)$  is related to the plastic deformation process inside this expanding volume fraction. According to eqn.(4) the mean free path of dislocation motion decreases with increasing strain from an initial value  $s_1$  to a final value  $s_0$  at a rate defined by the rate constant  $k$ . Within the present experimental conditions the final mean free path  $s_0$  is observed to be approximately independent of strain rate. At higher temperatures, however,  $s_0$ , usually decreases with decreasing temperature  $T$  and increasing applied strain rate.

In Fig. 5 a/ we can see that the initial mean free path,  $s_1$ , increases with increasing applied strain rate from a value of approximately  $0.8 \mu\text{m}$  to approximately  $3.5 \mu\text{m}$ . The following mathematical expression describes this relationship

$$s_1 = 6.06 \cdot 10^{-5} \cdot \dot{\epsilon}_0 + 7.78 \cdot 10^{-7} \quad (11)$$

An explanation for this behavior may be that an increase in strain rate causes  $f_1$  to increase and the local strain rate to decrease. Hence the rate of thermal activation inside the active volume fraction is increased. This in turn may make  $s_1$  increase.

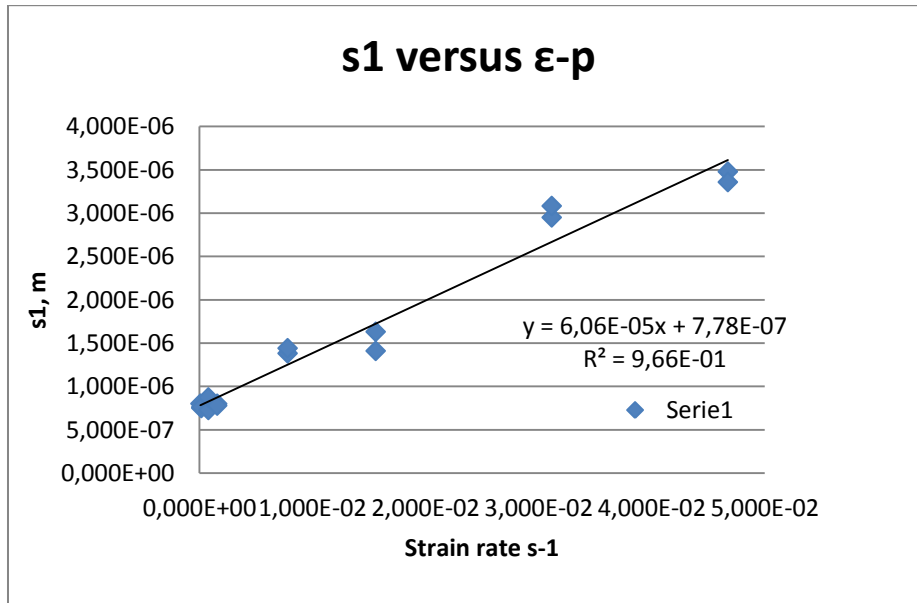


Fig.5a. s1 versus applied strain rate at T=296K

The rate constant k

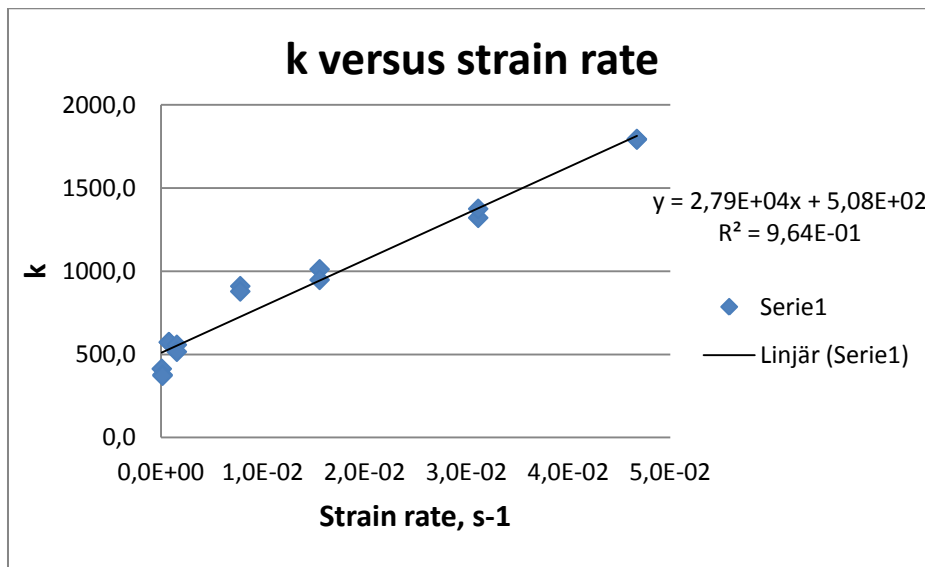


Fig.5b. k versus applied strain rate at T=296K

The strain rate dependence of this parameter is presented in Fig. 4b and it is obvious that k increases with increasing applied strain rate in accordance with the following mathematical expression:

$$k = 2.79 \cdot 10^4 \cdot \dot{\epsilon} + 5.08 \cdot 10^2 \quad (12)$$

The increase in k with applied strain rate presumably has a similar explanation as that for the increase in  $s_1$ , see above.

### The three stages of the plastic deformation process in DP600 steel

It has been suggested by several investigators (11) that the stress-strain curve of DP steel may be divided into at least three different stages. This type of behavior is also observed in the presently investigated DP600 steel when the stress-strain data are plotted in a  $\log \sigma$ - $\log \epsilon$  - diagram, see Fig. 3. We can see that Stage I ends after a strain of  $\approx 0.3\%$ . Stage II occurs in the strain interval  $\approx 0.3\% - 3\%$  and Stage III starts at 3% and continues to necking.

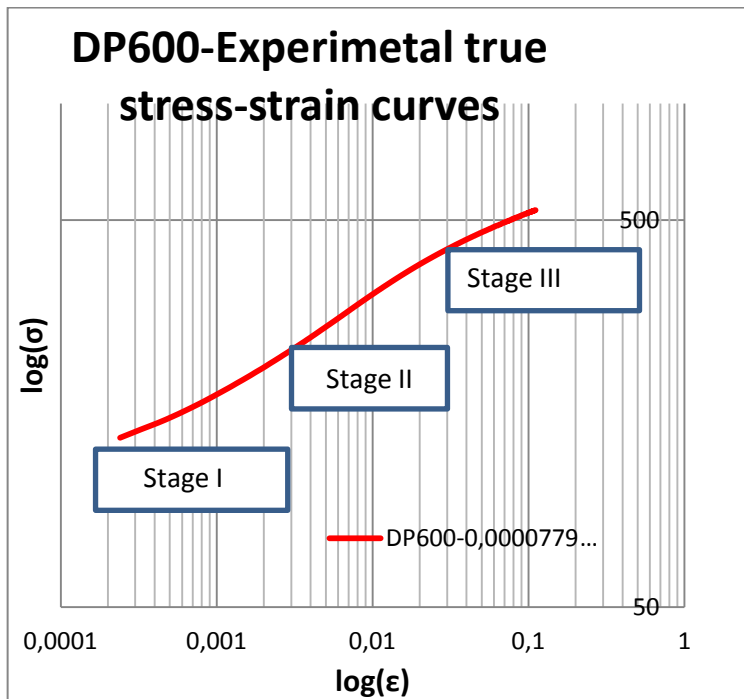


Fig. 6.  $\log \sigma$  -  $\log \epsilon$  plot of the stress-strain curve for DP600 steel tested at RT and a strain rate of  $0.000417\text{s}^{-1}$ . Stage I goes from zero strain to 0.3% strain. Stage II is between 0.3% and 3%. Stage III goes from 3% to necking.

In order to explain this behavior in terms of physical mechanisms we will analyze the strain dependences of the local strain rate  $\dot{\epsilon}(\epsilon)$ , the thermal friction stress  $\sigma^*(\epsilon)$ , the volume fraction of active ferrite,  $f(\epsilon)$ , and the mean free path,  $s(\epsilon)$ . These are the strain dependent factors influencing the work hardening process and, therefore, by plotting the strain dependence of these factors in  $\log$ - $\log$  diagrams it is reasonable to assume that the result would reveal which of the different factors controls which of the three different stages. The results from this type of plots are shown in Fig. 7a-d. The applied strain rate  $\epsilon_0$  is equal to  $0.000079\text{ s}^{-1}$  and the testing temperature is equal to 298K.

Fig. 7a shows the  $\log s(\epsilon) - \log \epsilon$  plot and, because of the high  $k$  - value,  $s$  very rapidly approaches its minimum value  $s_0$ . The blue point in the figure marks the inflexion point which appears at  $\epsilon \approx 0.3\%$ . Since the change in  $\log(s(\epsilon))$  is very small for strains above 1% of strain it is reasonable to assume that Stage I is closely related to the decrease in the mean free path of dislocation motion  $s(\epsilon)$  with strain.

Plots of the thermal friction stress,  $\sigma^*(\epsilon)$  and the active volume fraction  $f(\epsilon)$  versus strain in  $\log - \log$  diagrams, see Fig 7 b-c, both give inflexion points at the strain 3%. It is interesting to note that also the local strain rate has an inflexion point at 3% of strain which might indicate that Stage II is in fact

defined by the local variation in strain rate. This is so because both  $\sigma^*(\epsilon)$  and  $f(\epsilon)$  are strain rate dependent. Stage III, finally, is defined for strains larger than 3%.

A possible conclusion might therefore be that Stage I is defined by the strain dependence of the mean free path of dislocation motion while Stage II is defined by the local strain rate dependence in the strain interval 0.3% - 3%. Stage III occurs for strains larger than 3%

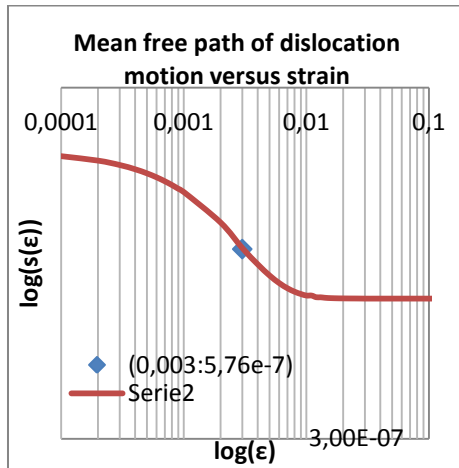


Fig.7a.  $\log s(\epsilon) - \log \epsilon$  The inflexion point is located at  $\epsilon \approx 0.3\%$ .

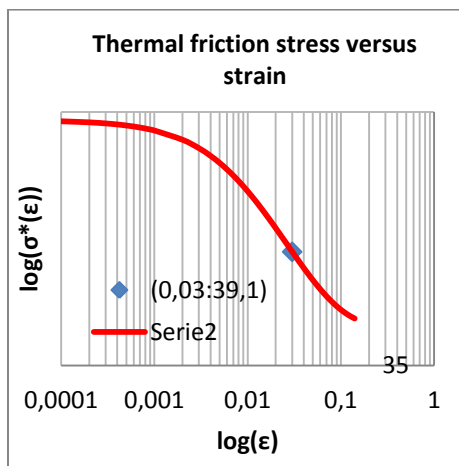


Fig. 7b.  $\log \sigma^* - \log \epsilon$  The inflexion point is located at 3%

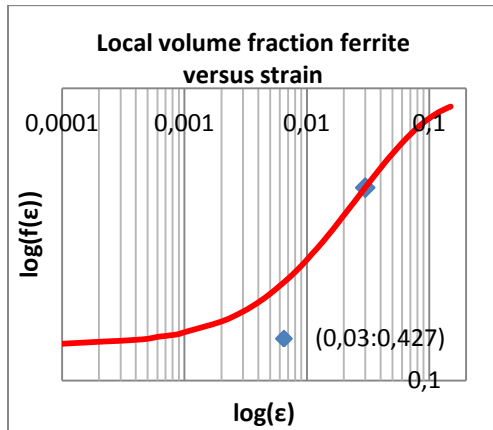


Fig. 7c.  $\log f(\epsilon) - \log \epsilon$  The inflexion point is located at 3%

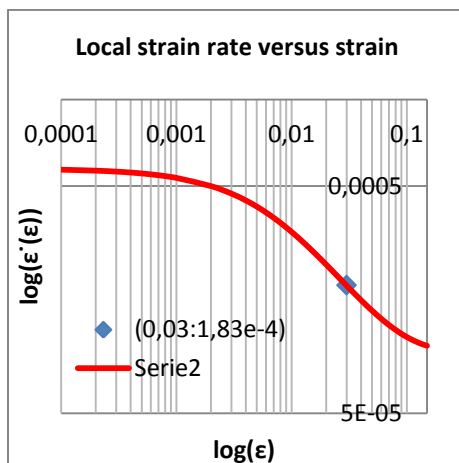


Fig. 7d.  $\log \dot{\epsilon}(\epsilon) - \log \epsilon$  The inflexion point is located at 3%

### The prediction of specimen temperature proceeding from the proposed model

It is well known that most of the energy transported to the material during plastic deformation is heat with a resulting temperature rise in the material. In the present theoretical analysis of the stress – strain behavior of DP600 steel we have used the presently proposed model to estimate the temperature rise in the testing specimens. In this analysis we assume that the increase in temperature  $\Delta T$  (K) may be written

$$\Delta T = \frac{Q}{C \cdot V} \quad (13)$$

Where  $Q$  is the added energy in J,  $C$  is the volumetric heat capacity ( $\frac{J}{cm^3 \cdot K}$ ) and  $V$  is the volume ( $cm^3$ ).

In order to calculate the value of  $Q$  we will proceed from the following expression

$$Q = \int_0^{0.1} \sigma(\varepsilon) \cdot d\varepsilon \quad (14)$$

and by using the integration limits 0 to 0.1 we obtain  $Q=65.8$  J for test specimen 1, see Table 1. The volume of the specimen is  $2.572 \text{ cm}^3$  and  $C=3.537$  for ferrite (tabulated data). By inserting these values into eqn.(13) we obtain  $\Delta T=7.23$ K. Now, assuming that the testing temperature was 25C and that all energy goes to a temperature rise the calculated specimen temperature would be 305.2K. The estimated average value is 306.8, see Table 2. The agreement is reasonably good.

The scatter in the T-values is however comparatively high and the procedure must be refined.

### The number of parameters involved in the proposed dislocation theory

There is no doubt that the work hardening of crystalline materials is one of the most complicated areas in modern physics. The reason for this is of course that many different factors and many different processes are involved. This also holds for the work hardening process in a simple uniaxial tensile test.

In the present dislocation theory a large number of parameters are involved. Some of these parameters are physically based constants while other parameters can be experimentally determined or verified. This for instance holds for the dislocation strengthening parameter,  $\alpha$ , the shear modulus  $G$ , the Burgers vector,  $b$ , the Taylor factor,  $m$ , the applied strain rate,  $\dot{\varepsilon}_0$ , the testing temperature,  $T$ , the volume fraction of ferrite,  $f_0$ , the volume fraction of martensite,  $f_m$ , the thermal friction stress,  $\sigma^*$ , in ferrite with the parameters coupled to this stress namely  $\sigma_0$ ,  $v$  and  $T_0$ . The values of the remaining six parameters, namely  $\sigma_{at}$ ,  $f_1$ ,  $r$ ,  $s_1$ ,  $s_0$  and  $k$  are however unknown. However, these six parameters have all a well defined physical meaning and the reasonableness of the obtained values can be checked in various ways. Some examples of these possibilities are the following:

#### Example 1

The DP600 steel does not exhibit a Lüders phenomenon. Hence the flow stress at 0.2% strain may be written

$$\sigma(0.002) = \sigma_{at} + \sigma^* + \alpha \cdot G \cdot b \cdot \sqrt{\rho(0.002)} \quad (15)$$

where  $\rho(0.002)$  may be estimated from the following simplification of eqn.(2)

$$\rho = \frac{m}{f_1 \cdot s_1 \cdot b} \cdot \varepsilon + \rho_0 \quad (16)$$

where the values of  $f_1$ ,  $s_1$  and  $\rho_0$  are given in Table 2 and  $m=2$  and  $b=2.5 \cdot 10^{-10}$  and  $\varepsilon=0.002$ . Inserting these values into eqn.(16) we obtain  $\rho(0.002)=3 \cdot 10^{14} \text{ m}^{-2}$  and from eqn.(15) that  $\sigma(0.002) \approx 422$  MPa. The corresponding experimental value for  $\sigma_{0.2\%}$  is 438MPa. The error is less than 4% which may be considered as a good agreement and indicates the reasonableness of the parameters involved.

#### Example 2

There is a strong correlation between the mean free path  $s_0$  of dislocation motion and the “grown-in” dislocation density  $\rho_0$  and according to Reid et al (14) it holds that

$$s_0 = K \cdot \rho_0^{-\frac{1}{2}} \quad (16)$$

where for DP steel  $K \approx 6$ . For the lowest strain rate (specimen 1) we have that  $\rho_0 = 1.48 \cdot 10^{14} \text{ m}^{-2}$ . According to eqn. (16) we then obtain that  $s_0 \approx 0.49 \text{ }\mu\text{m}$  which is close to the fitted value of  $0.5 \text{ }\mu\text{m}$ , see Table 2.

#### Example 3

It is also possible to estimate the value of the final mean free path,  $s_0$ , of dislocation motion by correlating it to the dislocation cell diameter. There are various techniques available for this purpose among which transmission electron microscopy may be mentioned.

#### Example 4

In the present investigation correlations have been observed between different parameters. This is illustrated in Fig. 8. where the rate constant  $r$  is plotted as a function of the initial active volume fraction  $f_1$ . It is quite obvious from the figure that a linear relationship exists between the two parameters according to the following equation

$$r = 28.12 - 72.56 \cdot f_1 \quad (17)$$

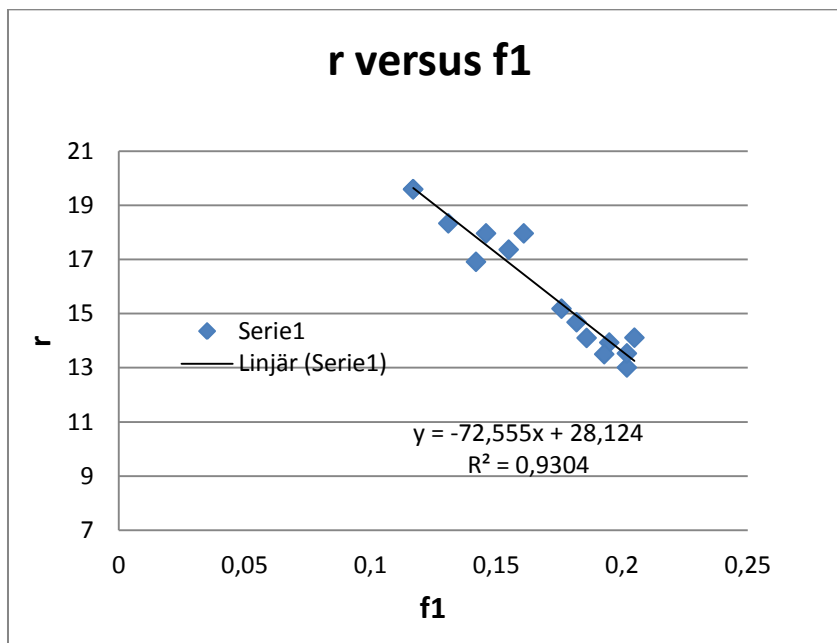


Fig. 8. Rate constant  $r$  versus initial volume fraction,  $f_1$

A similar relationship is observed between the rate constant  $k$  and the initial mean free path  $s_1$ . This is clearly illustrated by Fig. 9 and it is obvious that the following mathematical formula describes this connection

$$k = 4.48 \cdot 10^8 \cdot s_1 + 170 \quad (18)$$

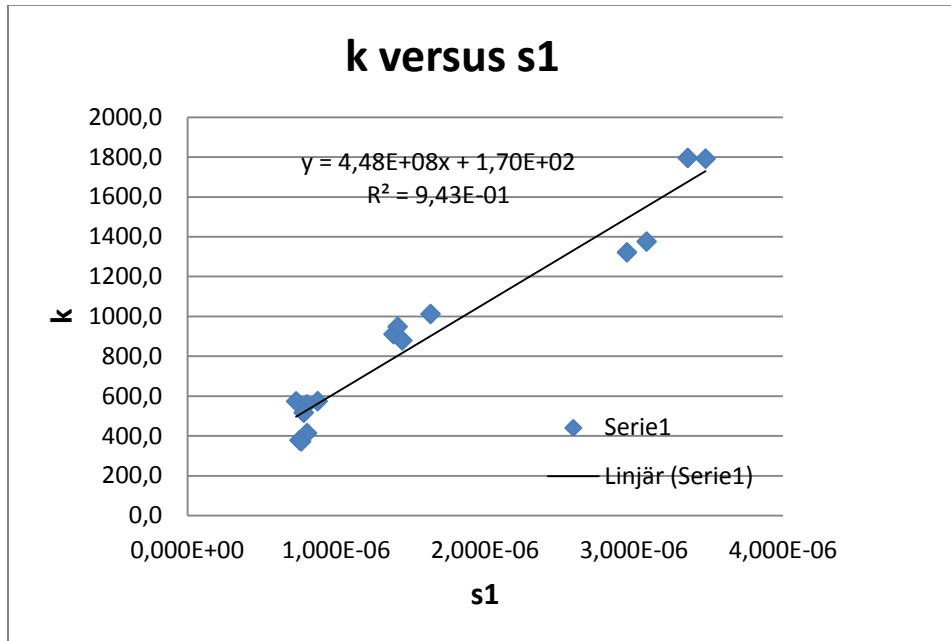


Fig. 9. Rate constant  $k$  versus initial mean free path,  $s_1$ , of dislocation motion

#### Example 5

There are also close mathematical relationships between  $f_1$ ,  $r$ ,  $s_1$  and  $k$  on the one side and  $\dot{\epsilon}_0$  on the other side, see Fig. 4 and Fig. 5.

#### Comments regarding examples 1 - 5

The example in Fig. 8 indicates that the two parameters  $r$  and  $f_1$  may be replaced by one parameter. A similar condition holds for the parameters  $k$  and  $s_1$ , see Fig. 9. This implies that the number of unknown parameters decreases from six to four. Together with the other four examples presented above it is obvious that the present theory opens for new possibilities to on the one hand increase our understanding of the work hardening process in DP steel and on the other hand to reduce the number of parameters involved.

#### Summary and conclusions

A recently presented dislocation based model for the work hardening behavior of DP steels is used to investigate the strain rate dependence of DP600 steel. Due to the expansion of the active volume fraction,  $f$ , with strain the thermal stress  $\sigma^*$ , and the local strain rate  $\dot{\epsilon}$  decreases with strain. For this purpose the strain rate dependence of thermal friction stress,  $\sigma^*$ , is taken into account. It should be observed that also the parameters  $f(\epsilon)$  and  $s(\epsilon)$  are strain rate dependent.

An attempt is also made to explain the three different stages of work hardening in this type of steel. Comments are given with respect to the number of parameters involved in the model and various ways to independently estimate the values of some of these parameters.

The following conclusions are drawn:

- The theory accurately describes the true stress-strain behavior of the investigated DP600 steel at all investigated strain rates
- The parameter values obtained in the fitting procedure are physically reasonable and in accordance with independent estimates.
- It is concluded that Stage I (0 – 0.3%) of straining is defined by the initial decrease of the mean free path,  $s$ , of dislocation motion. Stage II (0.3% - 3%) is directly caused by the strain rate dependence of the local strain rate,  $\dot{\epsilon}$ , and indirectly by the thermal friction stress,  $\sigma^*$ , and the local active volume fraction,  $f$ . Stage III (3% - necking) is mainly defined by the total amount of ferrite,  $f_0$ , the final mean free path of dislocation motion,  $s_0$ , and the dislocation remobilisation factor  $\Omega$ .
- In the present dislocation theory a large number of parameters are involved. Some of these parameters are physically based constants while other parameters can be experimentally determined. The values of the remaining six parameters, namely  $\sigma_{at}$ ,  $f_1$ ,  $r$ ,  $s_1$ ,  $s_0$  and  $k$  are unknown. However, these six parameters have all a well defined physical meaning and the reasonableness of the obtained values can be checked in various ways. In fact two of these parameters may according to the present analysis be eliminated resulting in only four independent parameters some of which can be experimentally checked.
- Since the temperature  $T$  is a variable in the proposed theory an attempt is made to estimate the specimen temperature increase due to the work carried during plastic deformation. The theoretically calculated value is 305.2 K while the average fitted value is 306.8 K. This is an acceptable result. The scatter in the fitted results is high and implies that this analysis must be refined.
- It seems that the present approach of analyzing the work hardening behavior of DP steel opens a new door for further development of DP steel as well as for other metals with a soft matrix containing hard particles. Preliminary results from an aluminum alloy containing 5% ceramic particles indicate that also Al-alloys may be analyzed with the proposed model.

## References

1. Taylor G. I., [http://en.wikipedia.org/wiki/Geoffrey\\_Ingram\\_Taylor](http://en.wikipedia.org/wiki/Geoffrey_Ingram_Taylor)
2. Polanyi M., [http://en.wikipedia.org/wiki/Michael\\_Polanyi](http://en.wikipedia.org/wiki/Michael_Polanyi)
3. Orowan E., [http://en.wikipedia.org/wiki/Egon\\_Orowan](http://en.wikipedia.org/wiki/Egon_Orowan)
4. Volterra V., [http://en.wikipedia.org/wiki/Vito\\_Volterra](http://en.wikipedia.org/wiki/Vito_Volterra)
5. Taylor G. I., Proc. Roy. Soc, 1934. A145: p. 362.
6. Mughrabi, H., Material Science and Engineering A, 2004. 387-389: p. 209-213
7. Bergström, Y., "The plastic deformation of metals – a dislocation model and its applicability. Reviews on powder metallurgy and physical ceramics. 1983. 2(2&3):p. 79-265
8. Bergström, Y., <http://plastic-deformation.com>
9. Rigsbee, J.M., et al., The Metallurgical Society of AIME, 1979: New Orleans.
10. Korzekwa, D.A., Matlock, D.K., and Krauss, G., Met. Trans. A, 1984, 15A:p. 1221-1228.
11. Liedl, U., Traint, S., and Werner, E.A. Computational Material Science, 2002. 25: p. 122-128.
12. Ashby, M.F., The deformation of plastically non-homogeneous alloys, ed. R.B.N. Kelly A. 1971, London: Applied Science Publishers LTD.
13. Bergström, Y., Granbom, Y., and Sterkenburg, D. Journal of Metallurgy, Volume 2010 (2010)

14. Reid, C.N., Gilbert, A.R., and Rosenfield, A.R., Phil. Mag. 12, 409(1965).